



Tetravalent Cerium Cation Imprinted Crosslinked Acrylamide/Alginic Acid Copolymer Network: A Sorption and Ce(IV) Ion-Selectivity Study from Aqueous Solutions

P. ROHITH^{1b}, SARASWATHI S. KUMAR^{1b} and P. GIRIJA*^{1b}

PG Department of Chemistry and Research Centre, Sanatana Dharma College, Alappuzha-688003, India

*Corresponding author: E-mail: girijakallelil@gmail.com

Received: 6 April 2023;

Accepted: 8 May 2023;

Published online: 6 July 2023;

AJC-21281

A novel tetravalent cerium cation-imprinted crosslinked polymer network (Ce(IV)-CICPN) based on polyacrylamide was synthesized by metal-ion-imprinting strategy in an aqueous medium with N,N-methylene-bis-acrylamide (NNMBA) as crosslinker. The synthesized CPN is characterized by UV-Vis spectroscopy, FTIR spectroscopy, PXRD analysis, SEM studies, EDX and thermogravimetric analysis. The adsorption performance was studied using adsorption isotherms and kinetics. The Ce(IV)-CICPN was optimized for maximum Ce(IV) ion sorption using the batch equilibration method, and its performance has been compared with that of a non-imprinted crosslinked polymer network (non-imprinted CPN). It was found that it possesses a maximum adsorption capacity of 70.3 mg/g. The surface area of both Ce(IV)-CICPN and non-imprinted CPNs were determined by BET surface area analysis and found to be 2.103 m² g⁻¹ and 0.62 m² g⁻¹, respectively. Polymer efficiency as a selective sorbent for Ce(IV) ion was estimated through examining its selectivity relative to Zn(II), Mg(II), Cr(IV) and V(V).

Keywords: Cerium, Cation-imprinted crosslinked polymer network, Sorbent, Selectivity.

INTRODUCTION

Metal ion imprinting technology is a novel method for synthesizing specific polymer networks imprinted with metal ions. This strategy uses the concept of supramolecular recognition, which enables the host polymer framework to pair with template metal ions based on their characteristics such as size, shape, functional groups present in them, etc. It enables to synthesize a new pattern-type molecular framework that possesses multifaceted applications in chromatographic separations, sensors, catalysis and *in vitro* diagnostics [1]. This metal ion imprinted polymer exhibits high selectivity and specificity towards the target metal ion species. This makes them more significant in the field of selective sorption of metal ions from their aqueous solutions. In the synthesis of metal ion-imprinted polymers, a template metal ion is used to synthesize a cross-linked polymer network with useful characteristics. Before polymerization, metal ions imprint their molecular pattern by forming a complex with a suitable ligand. They are found to be effective in sensors [2], solid phase extraction [3] and membrane separation [4].

Metal ion pollutants are one of the major threats to the environment nowadays. Metal ion-imprinted polymers can act as an effective sorbent to achieve the separation of metal ions in an environmentally and economically benign way. Among lanthanides, cerium in water is much more concerned due to its detrimental effects on aquatic flora and fauna. Even at micromolar concentration, cerium affects the embryogenesis of sea urchins by inducing cytogenic anomalies [5]. A reduction in photosynthetic pigments, disruption in nutrients and increase in malondialdehyde content were found as the toxic effects of cerium on *Elodea canadensis* [6].

Moussa *et al.* [7] prepared an ion-imprinted polymer using Nd³⁺ as template species using methacrylic acid as complexation monomer and ethylene glycol dimethacrylate (EGDMA) as the crosslinking agent with an ability to selectively extract lanthanide ions simultaneously including Ce(III) with a specific capacity of about 60 μmol/g. Rahman *et al.* [8] synthesized a cerium-ion-imprinted polymer with amidoxime as complexing agent; EGDMA and AIBN as the crosslinking agent and free radical initiator, respectively. Similarly, Chen *et al.* [9] used a cerium-ion-imprinted polymer to modify carbon

paste electrodes for the purpose of sensitive and selective determination of Ce(III) ions from aqueous solutions. The efficacy of metal ion imprinted polymers in recognizing and specifically adsorbing the target metal ions can be exploited in using them as an effective sorbent which may find industrially and environmental applications.

In present work, a tetravalent cerium cation-imprinted crosslinked polymer network (Ce(IV)-CICPN) was synthesized based on polyacrylamide with alginic acid as functional monomer, N,N-methylene-bis-acrylamide (NNMBA) as the crosslinking agent and potassium persulphate as the initiator for initiating the polymerization process. The characterization, rebinding condition optimization and selectivity study were performed.

EXPERIMENTAL

All the experiments were carried out using analytical and spectral-grade reagents. The monomers used in this study, namely acrylamide, alginic acid, cerium nitrate; the crosslinker NNMBA and the initiator potassium persulfate were obtained from NICE Chemicals, India. Fourier transform infrared (FT-IR) spectra of the Ce(IV)-CICPN and its Ce(IV) ion-complex were recorded between 4000-400 cm^{-1} using a Perkin Elmer 400 FT-IR spectrophotometer. UV-Vis Spectra of cerium cation-imprinted crosslinked polymer network (Ce(IV)-CICPN) and its Ce(IV) ion-complex; and the amount of metal ion adsorbed determination before and after binding was carried out using Shimadzu 1200 UV-Vis spectrophotometer. The SEM images and EDAX of Ce(IV)-CICPN and its Ce(IV) ion-complex were taken using JEOL JSM-6390 instrument. The XRD data of the samples were analyzed using Aeris Research benchtop X-ray diffractometer. The BET analysis of Ce(IV)-CICPN was carried out using BET surface area and pore size analyzer Altamira Instruments, Inc. using the static volumetric method. The thermogravimetric analysis was carried out using Simultaneous Thermal Analyzer STA 8000.

Synthesis of tetravalent cerium cation-imprinted cross-linked polymer network (Ce(IV)-CICPN): Tetravalent cerium cation-imprinted NNMBA crosslinked polymer network was prepared by the suspension polymerization method. Mixed 7.5 g alginic acid with 2 g ceric ammonium nitrate in 100 mL distilled water. To this mixture 10.6 g acrylamide, 0.3 g potassium persulphate and 7.71 g NNMBA were added. The polymerization was carried out with 70 °C with constant stirring. The Ce(IV)-CICPN obtained was washed with water to remove the unreacted monomer. The bulk polymer was dried, sieved and weighed. The non-imprinted analog of CPN was also prepared using the same procedure without cerium ion.

RESULTS AND DISCUSSION

UV-visible studies: In the UV-vis spectra of Ce(IV)-CICPN and Ce(IV) ion-complex of CPN, Ce(IV)-CICPN shows bands at 203 nm and 207 nm, which after binding of Ce(IV) ion shifted to 211 nm and 286 nm; may be as a result structural changes in the molecule. The wavelength of maximum absorption of Ce(IV)-CICPN at 203 nm was found to be shifted to 278 nm on binding of Ce(IV) ion on CPN. It is due to the inter-

action of Ce(IV) ion with the non-bonding electrons of the carboxylate group of alginic acid and might be due to $n \rightarrow \pi^*$ transitions. This information also reveals that the Ce(IV) ion has bound to the synthesized CPN [10].

FTIR studies: The spectra of the Ce(IV)-CICPN showed absorption at 3281.38 cm^{-1} which is due to the -OH stretching of alginic acid and shifted to 3344 cm^{-1} in Ce(IV) ion-complex of CPN. Also the C=O *str.* observed at 1639 cm^{-1} is found to be shifted to 1587 cm^{-1} . These observations divulges that the alginate carboxyl group participates in the Ce(IV) ion adsorption process through complexation. The peaks in the region below 1000 cm^{-1} can be due to the metal-oxygen bond in Ce(IV) ion-complex of crosslinked polymer network.

Powder XRD studies: The PXRD pattern of Ce(IV)-CICPN and its Ce(IV) ion-complex are shown in Fig. 1. The XRD pattern observed for Ce(IV)-CICPN shows main peaks at 13.44°, 20.82° and its Ce(IV) ion-complex shows peaks at the same 2 θ values and one at 28.97°. Thus, it can be understood that polymer matrix has not changed structurally on coordination with Ce(IV) ion and the peak obtained especially in the Ce(IV) ion-complex of CPN is due to the coordination of Ce(IV) on the imprinted polymer matrix.

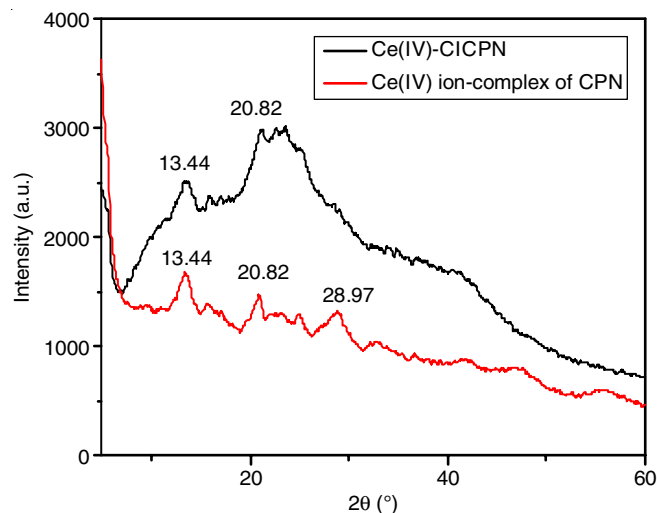


Fig. 1. Powder XRD pattern of Ce(IV)-CICPN and Ce(IV) ion complex of CPN

Thermal studies: The thermal decomposition behaviour of an ion-imprinted polymer network depends on the type of coordination geometry as well as the macromolecular characteristics of the polymer [11]. The TG and DTA plots of Ce(IV)-CICPN and its Ce(IV) ion-complex are shown in Fig. 2. The TG Plots depicts three stages of decomposition for Ce(IV)-CICPN and for its Ce(IV) ion-complex, it depicts two stages of decomposition. For Ce(IV)-CICPN, initially the water adsorbed on the CPN was removed. In first stage between the temperature range 166-267 °C, carboxylate groups are decomposed [12]. Thereafter the major decomposition comes in the range of 300-510 °C, which is attributed to the breakdown of the polymer backbone. In a similar way, for Ce(IV) ion-complex, initial decomposition stage is in the range 38-125 °C attributed to the decomposition of free or unbound carboxylate groups in

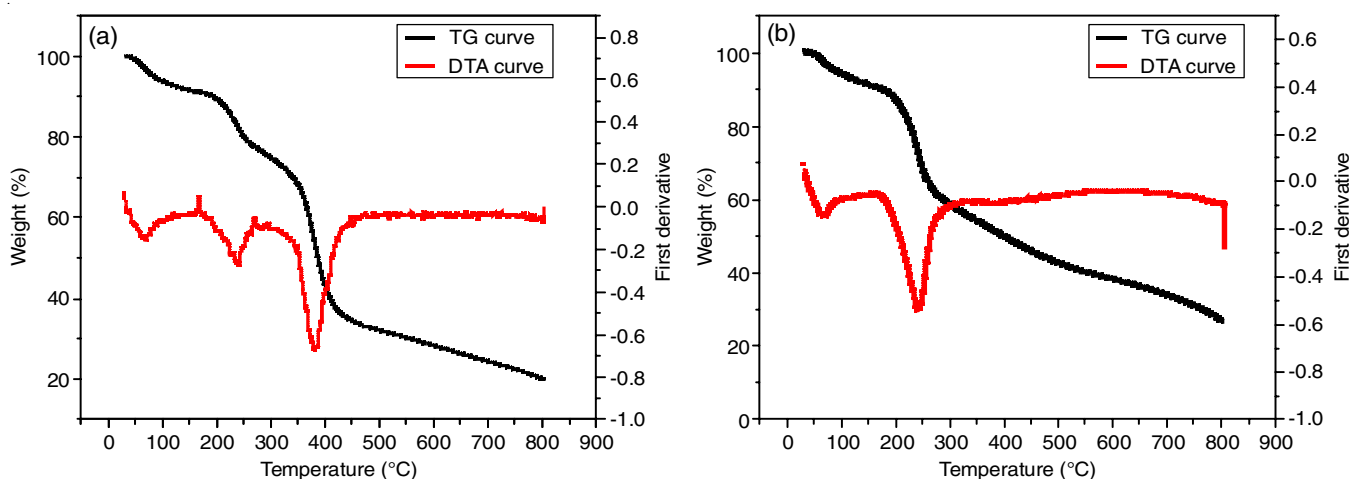


Fig. 2. TG and DTA plots of (a) Ce(IV)-CICPN (b) Ce(IV) ion complex of CPN

the complex and then the major decomposition in the temperature range 140-370 °C is due to the decomposition of polymer matrix leaving the Ce(IV) ion residue. It is revealed that the thermal stability of Ce(IV)-CICPN is much greater than its Ce(IV) ion-complex. The same inferences can be obtained from DTA plots. It depicts three endothermic and one endothermic peaks at 51.30, 223.59 and 374.45 °C and 157.14 °C, respectively for CPN and; two endothermic peaks at 55.62 and 228.78 °C for Ce(IV) complex of CPN. The major endothermic peaks are observed for 37.45 and 228.78 °C due to the decomposition of polymer backbone for Ce(IV)-CICPN and Ce(IV) ion-complex of CPN, respectively.

SEM studies: The surface morphological analysis of both Ce(IV)-CICPN and its Ce(IV) ion-complex was performed by taking scanning electron microscope (SEM) images (Fig. 3). On comparing both that are taken under the same condition, it can be observed that the surface character of Ce(IV)-CICPN is completely changed on binding with Ce(IV) ions. It can be considered as evidence for the successful binding of Ce(IV) ions on the imprinted polymer sorbent.

EDX studies: The elemental composition and successful incorporation of Ce(IV) ions on the Ce(IV)-CICPN was investigated and substantiated by performing energy dispersive X-ray

analysis (EDX). EDX analysis of both Ce(IV)-CICPN and its Ce(IV) ion-complex are shown in Fig. 4. It can be inferred that Ce(IV) ion are completely absent in Ce(IV)-CICPN which can be considered as a strong piece of evidence for the successful synthesis of polymer with full functionality. Cerium(IV) ion incorporation on the cavities possessed by the synthesised CPN is confirmed by the EDX spectrum of Ce(IV) ion-complex of CPN, and the effectiveness of CPN as sorbent for Ce(IV) ions is established.

Optimization of effects of factors affecting sorption of Ce(IV) ion by Ce(IV)-CICPN and non-imprinted CPNs: Various factors affecting the sorption efficiency of Ce(IV)-CICPN such as initial concentration of Ce(IV) ion solution, time of contact and weight of polymer were optimized by batch equilibration method and the amount of Ce(IV) sorption is compared with that of non-imprinted CPN.

Effect of initial concentration on Ce(IV) ion sorption: The effect of the initial concentration of Ce(IV) ion on sorption was investigated by varying the initial concentration of Ce(IV) ion in the solution. The Ce(IV)-CICPN and non-imprinted CPN are equilibrated with Ce(IV) ion (20 mL, 0.02-0.007 N) and the concentration of Ce(IV) ion in solution before and after the binding was determined by means of UV-Vis spectroscopic method.

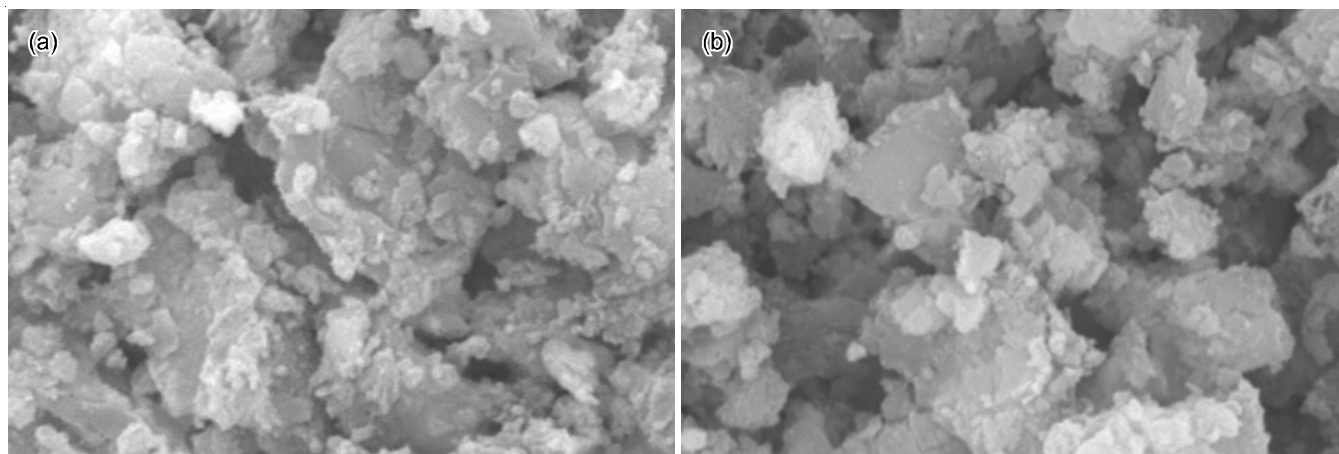


Fig. 3. SEM images of (a) Ce(IV) ion imprinted CPN (b) Ce(IV) ion complex of CPN

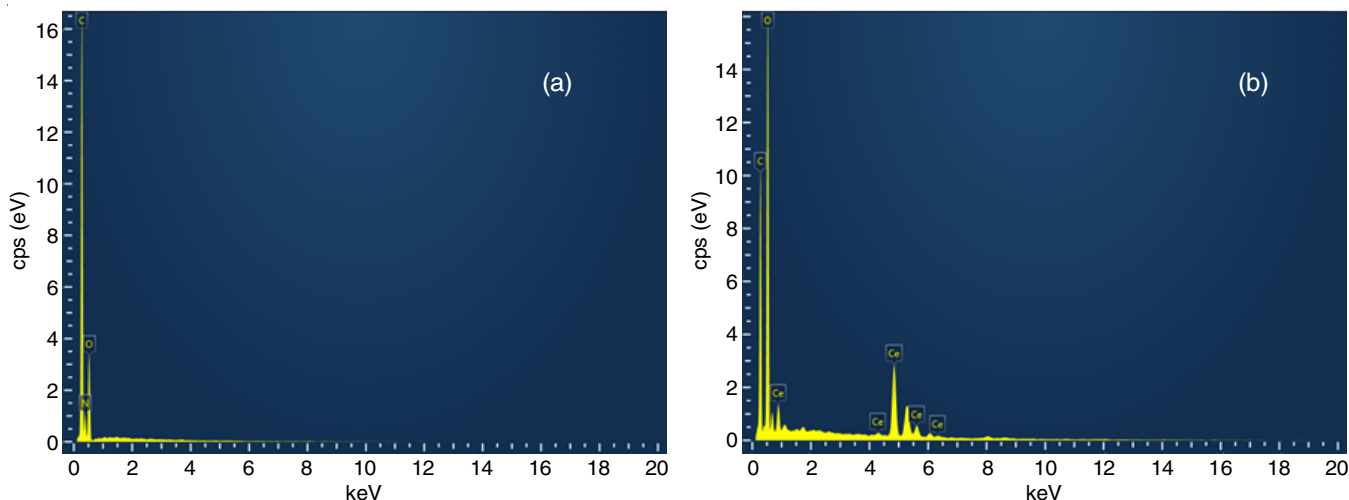


Fig. 4. EDX Spectrum of (a) Ce(IV)-CICPN (b) Ce(IV) ion complex of CPN

At lower concentrations, Ce(IV) ions are “site isolated” as suggested by Paczkowski & Neckers [13]. But at higher concentration, Ce(IV) ions are closer to each other and the repulsion between them are effectively controlled by the extent of crosslinked polymer [14]. It is suggested that all available active sites on the polymers will be utilized at higher concentrations [15]. As a result of the increased competition between Ce(IV) ions for vacant active sites, the sorption of Ce(IV) ions also increases proportionally. From Fig. 5, the Ce(IV) ion uptake increases with increases in concentration for Ce(IV)-CICPN compared to non-imprinted CPN and is due to more number of active sites vacated by imprinted Ce(IV) ions. The concentration study was proceeded further until maximum adsorption capacity is achieved and calculated as 70.3 mg/g.

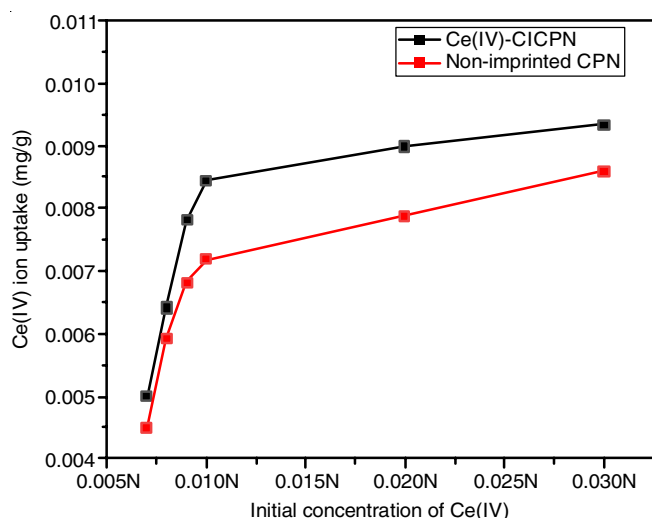


Fig. 5. Effect of initial concentration on Ce(IV)-CICPN and non-imprinted CPN

Effect of time of contact on Ce(IV) ion sorption: The batch equilibration method was carried out using 100 mg of Ce(IV)-CICPN and non-imprinted CPNs with (20 mL, 0.01 N) Ce(IV) ion solution to study the dependence of time of contact on the sorption of Ce(IV) ions. The Ce(IV) ions uptake is determined as a function of time by UV-vis spectrophotometric method.

In Fig. 6, initially, the Ce(IV) ion uptake was rapid rate and then attains equilibrium after 30 min by Ce(IV)-CICPN while non-imprinted CPN attains the same after 35 min. Thus the time for maximum adsorption is 30 min for Ce(IV)-CICPN while that for non-imprinted CPN is 35 min. The initial increase was due to the availability of more number of active vacant sites which gradually decreases as they are occupied. As a result, the optimum time interval of contact was found to be between 0-30 min for Ce(IV)-CICPN and between 0-35 min for non-imprinted CPN [16].

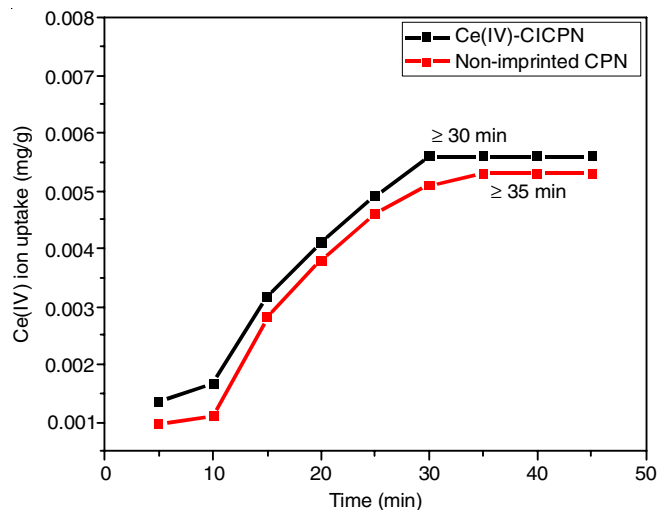


Fig. 6. Effect of time of contact on Ce(IV)-CICPN and non-imprinted CPN

Effect of weight of polymer: Different weights (50 to 150 mg) of Ce(IV)-CICPN was shaken with (20 mL, 0.03 N) Ce(IV) ion solution for 30 min. It is inferred that the amount of uptake of Ce(IV) ions by Ce(IV)-CICPN shows a decrease with an increase in the weight of the polymer loaded (Fig. 7). It is attributed to the aggregation of active sites, thereby decreasing the total surface area and increasing the adsorption path length [17].

Adsorption isotherm: Adsorption isotherms are useful in explaining the interaction of adsorbate species with the

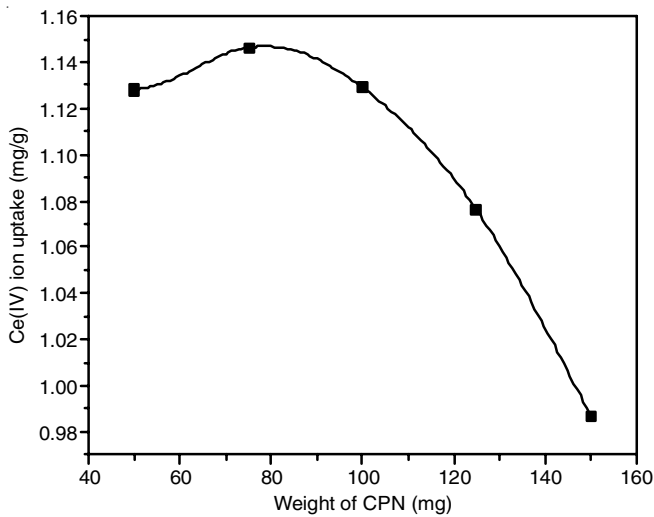


Fig. 7. Effect of weight of polymer

adsorbent system and describing the equilibrium distribution of adsorbate species on the adsorbent surface. Adsorption studies were carried out at different initial concentrations of Ce(IV) ions and analyzed by two adsorption models *viz.* Langmuir and Freundlich adsorption isotherms.

Langmuir isotherm: Langmuir adsorption isotherm can be used to describe the equilibrium between adsorbent and adsorbate systems, where adsorption is limited to monolayer at or before a relative pressure of unity is reached [18].

Langmuir model is represented by eqn. 1 [19]:

$$\frac{C_e}{q_e} = \frac{C_e}{q_m} + \frac{1}{K_L q_e} \tag{1}$$

where C_e (mg/L) is the equilibrium concentration Ce(IV) ions, q_e (mg/g) is the amount of Ce(IV) ions adsorbed at equilibrium, q_m (mg/g) is the maximum adsorption capacity, K_L (L/mg) is the Langmuir constant. A linear plot is obtained on plotting:

$$\frac{C_e}{q_e} \text{ vs. } C_e$$

Freundlich adsorption isotherm: Freundlich adsorption isotherm is an empirical adsorption isotherm model in which

the adsorbate forms a monolayer on the adsorbent surface. The adsorption isotherm is given by eqn. 2:

$$q_e = K_F C_e^{1/n} \tag{2}$$

The linear logarithmic form of eqn. 2 is represented as:

$$\ln q_e = \ln K_F + \frac{1}{n} \ln C_e \tag{3}$$

where C_e (mg/L) is the equilibrium concentration Ce(IV) ions, q_e (mg/g) is the amount of Ce(IV) ions adsorbed at equilibrium, K_F and n are Freundlich constants related to adsorption capacity and intensity, respectively [19,20]. In Freundlich adsorption isotherm, a linear plot is obtained on plotting $\ln q_e$ vs. $\ln C_e$.

The values of K_F and n can be determined from the intercept and slope of the isotherm. The adsorption of Ce(IV) ions on the Ce(IV)-CICPN is analyzed using Langmuir and Freundlich adsorption models at room temperature. Fig. 8a shows the Langmuir adsorption isotherm for the adsorption of Ce(IV) ions on the NNMBA crosslinked IPN gel, but was found to be given an unfair regression value of 0.7703. Fig. 8b shows the Freundlich adsorption isotherm obtained by plotting $\ln q_e$ vs. $\ln C_e$, with a fair linear regression value of 0.9971. It affirms that the adsorption of Ce(IV) ions on the Ce(IV)-CICPN gel follows Freundlich adsorption model at room temperature. From the plot (Fig. 9), values of K_F and n are determined as 3.0776 and 0.5324, respectively.

Surface and pore characterization: The Brunauer-Emmett-Teller (BET) surface analysis was performed by static volumetric method with both Ce(IV)-CICPN and non-imprinted CPN. The Ce(IV)-CICPN exhibits a specific surface area of 2.103 m²/g while that of non-imprinted CPN is 0.62 m²/g [21]. Also the pore size on Ce(IV)-CICPN was found to be of 11.09 nm in diameter. These cavities on the surface of Ce(IV)-CICPN are formed due to the removal of Ce(IV) ions and this porosity is the cause of higher surface area presented by Ce(IV)-CICPN than of non-imprinted CPN.

Adsorption kinetic studies: The adsorption kinetics was investigated by following the time-dependent adsorption of Ce(IV) ions by Ce(IV)-CICPN. A fixed mass of Ce(IV)-CICPN was equilibrated with (20 mL, 0.01N) Ce(IV) ion solution

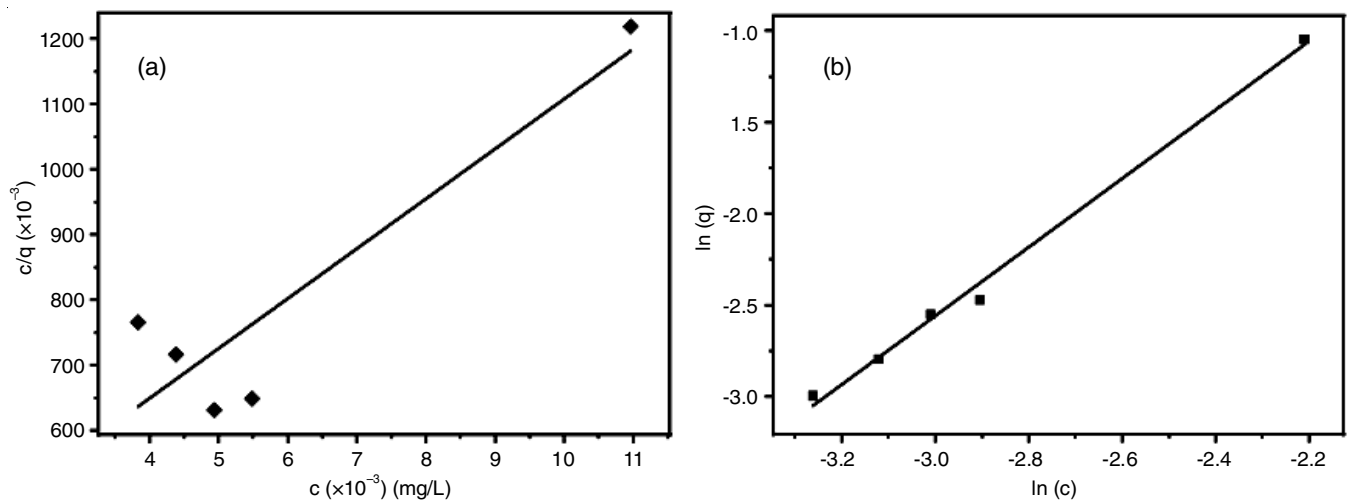


Fig. 8. Adsorption isotherm (a) Langmuir (b) Freundlich

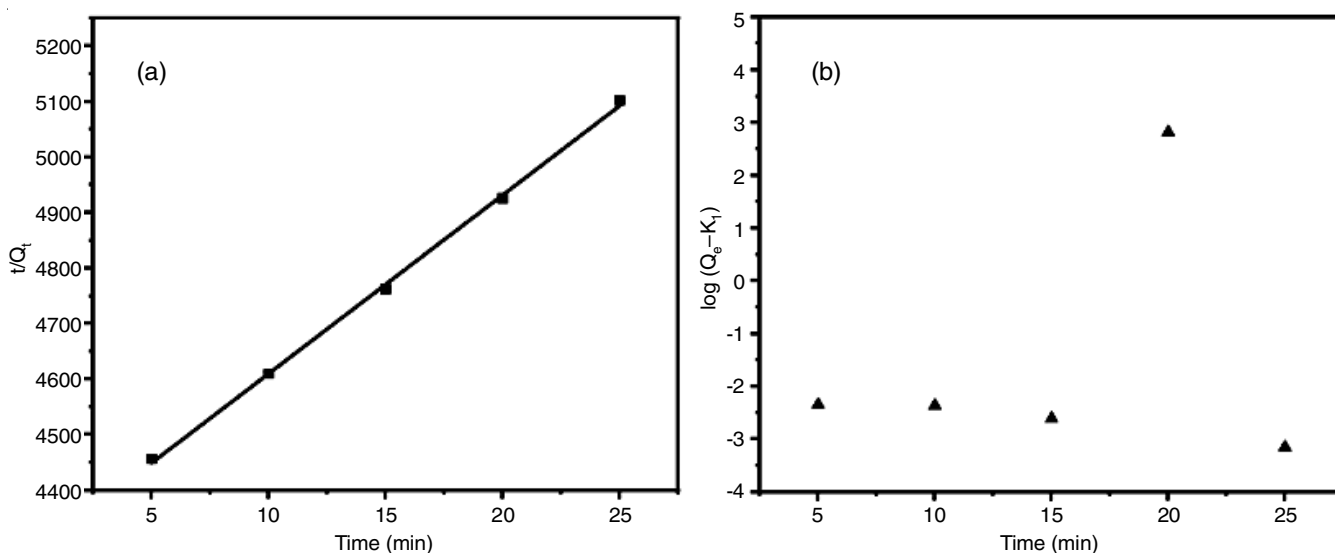


Fig. 9. Adsorption kinetics (a) pseudo-first order model (b) pseudo-second order model

and Ce(IV) ion uptake was determined as a function of time. The data was analyzed by pseudo-first order and pseudo-second order kinetic models [22].

Pseudo-first order kinetic equation is represented as [23]:

$$\frac{dQ_e}{dt} = K_1(Q_e - Q_t) \quad (4)$$

where Q_e and Q_t are the amount of uptake of Ce(IV) ions in mg/g at equilibrium and at a particular time t respectively. $K_1 \text{ min}^{-1}$ is the pseudo-first order rate constant [24].

On integrating eqn. 1 for boundary conditions:

$$\log\left(\frac{Q_e}{Q_e - Q_t}\right) = \frac{\log(Q_e - K_1)t}{2.303} \quad (5)$$

From eqn. 5 [20], the values of K_1 and Q_e can be determined from the slope and y-intercept of the linear plot of $\log(Q_e - K_1)$ against t .

The pseudo-second order kinetic equation is represented as [23]:

$$\frac{dQ_e}{dt} = K_2(Q_e - Q_t)^2 \quad (6)$$

where Q_e and Q_t are the amount of uptake of Ce(IV) ions in mg/g at equilibrium and at a particular time t respectively. K_2 is the pseudo-second order rate constant. On integrating and linearized the eqn. 6 becomes:

$$\frac{1}{Q_t} = \frac{1}{K_2 Q_e^2} + \frac{1}{Q_e t} \quad (7)$$

Using eqn. 7 [20], the values of K_2 and Q_e can be determined from the slope and y-intercept of the linear plot of t/Q_t against t .

Plots were analyzed to validate pseudo-first order and pseudo-second order kinetic models (Fig. 9) and the results are given in Table-1. As from the values of correlation coefficient (r^2) in Table-1, the adsorption of Ce(IV)-CICPN can be better explained by pseudo-first order kinetic model.

TABLE-1
CHARACTERISTIC VALUES OF
ADSORPTION KINETIC MODEL PLOTS

Kinetic model	r^2	Rate constant (min^{-1})
Pseudo first order model	0.9990	32.1667
Pseudo second order model	0.0529	0.0714

Water adsorption studies: The water adsorption ability of polymer depends on the nature of its polymer backbone, its chemical character and the extent of crosslinking. A good solvent can bring the polymer to a state of complete solvation and thereby it can expand to form a gel. This extent of water adsorption can influence the uptake of ions by the ion-imprinted polymer [17]. The water adsorption behaviour of the Ce(IV)-CICPN and non-imprinted CPNs was investigated by making a time-bound study of its adsorption of water and determining its equivalent water adsorbed (EWA) percentage values using eqn. 8 [25] and found to be 31.70% and 39.24%, respectively.

$$\text{EWA (\%)} = \frac{W_t - W_o}{W_o} \times 100 \quad (8)$$

where W_t and W_o are the weight of the swollen CPN after time $t = 24 \text{ h}$ and the weight of dry CPN at time $t = 0$.

The maximum swelling was obtained for Ce(IV)-CICPN compared to its non-imprinted analog. It is due to the higher sorption of water molecules on the sites vacated by Ce(IV) ions even though have smaller EWA% value due to the extent of crosslinking; while in non-imprinted CPN EWA % is less due to lesser availability of surface sites for adsorption of water [21].

Selectivity studies: Selective affinity towards template species is investigated by competitive adsorption studies under the optimum conditions. 0.2 g of Ce(IV)-CICPN is equilibrated with (40 mL, 0.03 N) ternary solutions containing Ce(IV) ion along with Zn(II), Mg(II), Cr(VI) and V(V) separately for 30 min. After adsorption equilibrium was reached, the amount of Ce(IV) ion and the competing ion in each corresponding solutions were determined. From the results (Fig. 10), it could

TABLE-2
COMPARITIVE STUDY

Monomer(s)	Crosslinking agent	Method of polymerization	Adsorption capacity (mg/g)	Ref.
Chitosan	KH-560	Condensation polymerization	43.00	[26]
Acrylamide	EGDMA	Free radical polymerization	67.80	[27]
Chitosan, PVP	–	–	38.24	[28]
Acrylamide, alginic acid	NNMBA	Free radical polymerization	70.30	Present work

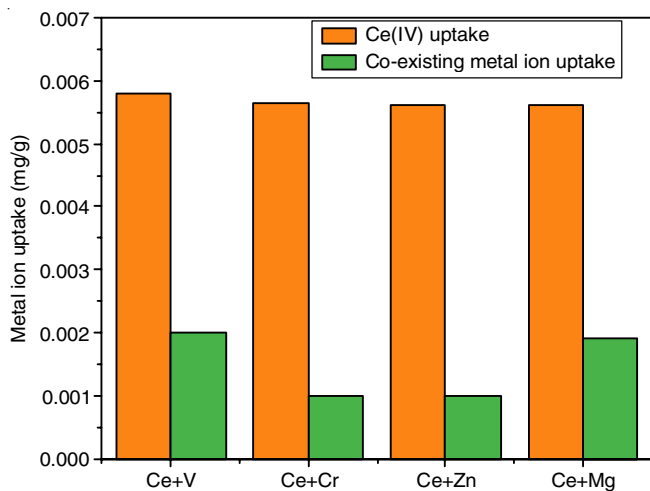


Fig. 10. Selectivity study

be concluded that the can be used as a suitable sorbent for the selective sorption of Ce(IV) ions from aqueous solutions.

Reusability studies: Reusability of the prepared Ce(IV)-CICPN without compromising its sorption efficiency was studied by elution method using (5 mL, 3 N HCl) as eluent. From the results (Fig. 11), it could be concluded that Ce(IV)-CICPN could be used upto 7 cycles by retaining its efficiency appreciably.

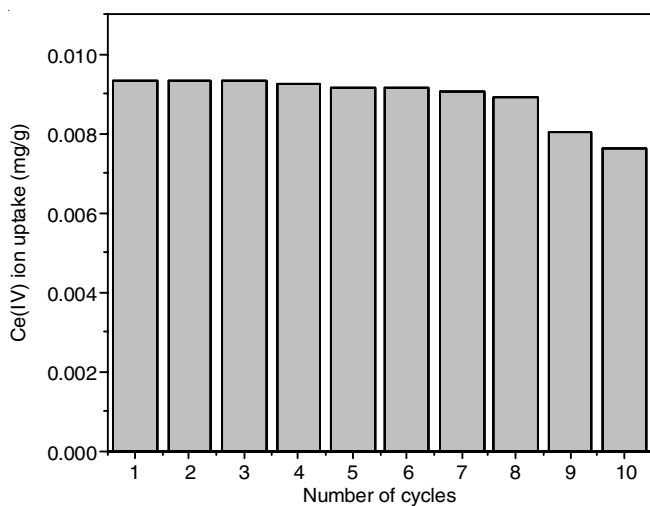


Fig. 11. Reusability study

Comparative study: Various cerium ion-imprinted polymer for the sorption and selective determination of cerium ions are reported earlier. Certain of these are compared in Table-2 with that in the present work based on their adsorption capacity. From the result of this study, it can be concluded that Ce(IV)-

CICPN can be an efficient sorbent for Ce(IV) ions compared to other reported works.

Conclusion

The present study comprises that Ce(IV)-CICPN is an effective material for the adsorption-based selective removal of Ce(IV) ions from aqueous solutions. From the characterization data, it could be inferred that the synthesized polymer could deliver the desired application. The optimization of sorption conditions helps to analyze the effect of various factors like concentration, time of contact and weight of polymer on efficient sorption of Ce(IV) ions and found that the maximum sorption occurs at higher concentration, at a lower weight of polymer loaded with a time of contact of 30 min. The concentration study reveals the maximum adsorption capacity of Ce(IV)-CICPN and found to be equal to 70.3 mg/g, which is much higher compared to other reported works. Adsorption isotherm studies of the sorption were validated by both Langmuir and Freundlich adsorption model and sorption kinetics was verified using pseudo-first and pseudo-second order model. From the validation studies, it unveils that sorption of Ce(IV) ions by Ce(IV)-CICPN can be better explained by Freundlich adsorption isotherm and follows pseudo-first order kinetics. The selectivity and reusability studies revealed that the produced Ce(IV)-CICPN may be employed as a selective sorbent for Ce(IV) ions from aqueous solutions without lowering its effectiveness up to 7 cycles.

CONFLICT OF INTEREST

The authors declare that there is no conflict of interests regarding the publication of this article.

REFERENCES

- L. Chen, X. Wang, W. Lu, X. Wu and J. Li, *Chem. Soc. Rev.*, **45**, 2137 (2016); <https://doi.org/10.1039/C6CS00061D>
- Z. Dahaghin, P.A. Kilmartin and H.Z. Mousavi, *Food Chem.*, **303**, 125374 (2020); <https://doi.org/10.1016/j.foodchem.2019.125374>
- J. Otero-Romani, A. Moreda-Pineiro, P. Bermejo-Barrera and A. Martin-Esteban, *Anal. Chim. Acta.*, **630**, 1 (2008); <https://doi.org/10.1016/j.aca.2008.09.049>
- Y. Zhai, Y. Liu, X. Chang, X. Ruan and J. Liu, *React. Funct. Polym.*, **68**, 284 (2008); <https://doi.org/10.1016/j.reactfunctpolym.2007.08.013>
- G. Pagano, M. Guida, A. Siciliano, R. Oral, F. Koçbas, A. Palumbo, I. Castellano, O. Migliaccio, P.J. Thomas and M. Trifuoggi, *Environ. Res.*, **147**, 453 (2016); <https://doi.org/10.1016/j.envres.2016.02.031>
- Y. Ma, J. Wang, C. Peng, Y. Ding, X. He, P. Zhang, N. Li, T. Lan, D. Wang, Z. Zhang, F. Sun, H. Liao and Z. Zhang, *Ecotoxicol. Environ. Saf.*, **134**, 226 (2016); <https://doi.org/10.1016/j.ecoenv.2016.09.006>

7. M. Moussa, M.M. Ndiaye, T. Pinta, V. Pichon, T. Vercoouter and N. Delaunay, *Anal. Chim. Acta*, **963**, 44 (2017); <https://doi.org/10.1016/j.aca.2017.02.012>
8. M.L. Rahman, P.Y. Puah, M.S. Sarjadi, S.E. Arshad, B. Musta and S.M. Sarkar, *J. Nanosci. Nanotechnol.*, **19**, 5796 (2019); <https://doi.org/10.1166/jnn.2019.16538>
9. J. Chen, H. Bai, J. Xia, X. Liu, Y. Liu and Q. Cao, *J. Rare Earths*, **36**, 1121 (2018); <https://doi.org/10.1016/j.jre.2018.03.014>
10. P. Girija and B. Mathew, *J. Chem. Chem. Eng.*, **7**, 508 (2013).
11. G. Parameswaran and B. Mathew, *Adv. Environ. Chem.*, **2014**, 394841 (2014); <https://doi.org/10.1155/2014/394841>
12. N. Sebastian, B. George and B. Mathew, *Polym. Degrad. Stab.*, **60**, 371 (1998); [https://doi.org/10.1016/S0141-3910\(97\)00095-5](https://doi.org/10.1016/S0141-3910(97)00095-5)
13. J. Paczkowski and D.C. Neckers, *Macromolecules*, **18**, 1245 (1985); <https://doi.org/10.1021/ma00148a035>
14. M.G. Gigimol and B. Mathew, *J. Appl. Polym. Sci.*, **104**, 2856 (2007); <https://doi.org/10.1002/app.25970>
15. V.P. Mahida and M.P. Patel, *Arab. J. Chem.*, **9**, 430 (2016); <https://doi.org/10.1016/j.arabjc.2014.05.016>
16. A.G. Ibrahim, F.A. Hai, H.A. Wahab and H. Mahmoud, *Am. J. Appl. Chem.*, **4**, 221 (2016); <https://doi.org/10.11648/j.ajac.20160406.12>
17. A. Aravind and B. Mathew, *J. Macromol. Sci., Part A Pure Appl. Chem.*, **57**, 256 (2020); <https://doi.org/10.1080/10601325.2019.1691451>
18. X. Luo and F. Deng, *Nanomaterials for the Removal of Pollutants and Resource Reutilization*, Elsevier (2018).
19. V.O. Njoku, K.Y. Foo, M. Asif and B.H. Hameed, *Chem. Eng. J.*, **250**, 198 (2014); <https://doi.org/10.1016/j.cej.2014.03.115>
20. R.L. Jose, M.G. Gigimol and B. Mathew, *Asian J. Chem.*, **32**, 311 (2020); <https://doi.org/10.14233/ajchem.2020.22338>
21. P. Girija and M. Beena, *Sep. Sci. Technol.*, **49**, 1053 (2014); <https://doi.org/10.1080/01496395.2013.866682>
22. L. Largitte and R. Pasquier, *Chem. Eng. Res. Des.*, **109**, 495 (2016); <https://doi.org/10.1016/j.cherd.2016.02.006>
23. E. Passaglia, M. Bertoldo, S. Coiai, S. Augier, S. Savi and F. Ciardelli, *Polym. Adv. Technol.*, **19**, 560 (2008); <https://doi.org/10.1002/pat.1107>
24. N. Ertugay and F.N. Acar, *Arab. J. Chem.*, **10**, S1158 (2017); <https://doi.org/10.1016/j.arabjc.2013.02.009>
25. E.F. Demir, E. Özçaliskan, H. Karakas, M. Uygun, D.A. Uygun, S. Akgöl and A. Denizli, *J. Biomater. Sci. Polym. Ed.*, **29**, 2218 (2018); <https://doi.org/10.1080/09205063.2018.1534423>
26. X. Zhang, C. Li, Y. Yan, J. Pan, P. Xu and X. Zhao, *Mikrochim. Acta*, **169**, 289 (2010); <https://doi.org/10.1007/s00604-010-0352-y>
27. Y. Hua, S. Zhang, H. Min, J.Y. Li, X.H. Wu, D. Sheng, X.B. Cui, Y.J. Chen, C. Li, H.Z. Lian and S. Liu, *At. Spectroscopy*, **42**, 217 (2021); <https://doi.org/10.46770/AS.2021.027>
28. I.M. Ali, E.S. Zakaria, M. Khalil, A. El-Tantawy and F.A. El-Saied, *J. Mol. Liq.*, **356**, 119058 (2022); <https://doi.org/10.1016/j.molliq.2022.119058>